Published in final edited form as:
J Phys Chem B. 2010 May 27; 114(20): 6968–6972. doi:10.1021/jp100039p.

Structural Assignment of 6-Oxy Purine Derivatives through Computational Modeling, Synthesis, X-ray Diffraction, and Spectroscopic Analysis

Xinyun Zhao[a,b], **Xi Chen**[a,b], **Guang-Fu Yang**[a], and **Chang-Guo Zhan**[b,*]

[a]Key Laboratory of Pesticide and Chemical Biology of the Ministry of Education of China, College of Chemistry, Central China Normal University, Wuhan 430079, P. R. China

[b]Department of Pharmaceutical Sciences, College of Pharmacy, University of Kentucky, 725 Rose Street, Lexington, KY 40536

Abstract

6-Oxy purine derivatives have been considered as potential therapeutic agents in various drug discovery efforts reported in literature. However, the structural assignment of this important class of compounds has been controversy concerning the specific position of a hydrogen atom in the structure. To theoretically determine the most favorable type of tautomeric form of 6-oxy purine derivatives, we have carried out first-principles electronic structure calculations on the possible tautomeric forms (**A**, **B**, and **C**) and their relative stability of four representative 6-oxy purine derivatives (compounds **1** to **4**). The computational results in both the gas phase and aqueous solution clearly reveal that the most favorable type of tautomeric form of these compounds is **A** in which a hydrogen atom bonds with N1 atom on the purine ring. To examine the computational results, one of the 6-oxy purine derivatives (*i.e.* compound **4**) has been synthesized and its structure has been characterized by X-ray diffraction and spectroscopic analysis. All of the obtained computational and experimental data are consistent with the conclusion that the 6-oxy purine derivative exists in tautomer **A**. The conclusive structural assignment reported here is expected to be valuable for future computational studies on 6-oxy purine derivative binding with proteins and for computational drug design involving this type of compounds.

Keywords

Purine derivative; molecular structure; quantum chemical calculation

Introduction

Purine derivatives are widely used as the common core structures in design and synthesis of lead compounds for drug discovery. Depicted in Scheme 1 are the common core structures of the 6-oxy purine derivatives, with four representative compounds (**1** to **4**). A variety of compounds with the common core structures have been identified as potentially valuable therapeutic agents, such as specific immunomodulators,1 antiviral agents,2 inhibitors of

*Correspondence: Chang-Guo Zhan, Ph.D. Professor, Department of Pharmaceutical Sciences, College of Pharmacy, University of Kentucky, 725 Rose Street, Lexington, KY 40536, TEL: 859-323-3943, FAX: 859-323-3575, zhan@uky.edu .

Supporting Information Available. Two figures for ^{1}H NMR and IR spectra of compound **4**. This material is available free of charge via the Internet at http://pubs.acs.org.

Multidrug Resistance Protein 4,[3] and phosphodiesterase 2 (PDE2), for the treatment of inflammation, thromboembolism, and diseases of cardiovascular or urogenital system.[4]

Although a variety of 6-oxy purine derivatives have been synthesized and their biological activities have been tested, the structural assignment of the compounds with these common core structures has been controversy. For example, the hydrogen atom was assigned to N1 atom on the purine ring (structure **A** in Scheme 1) in some reports.[5,6,7] However, in other reports, [8–10] the hydrogen atom was assigned to O10 atom (structure **B**, including **B-1** and **B-2**, in Scheme 1). According to another study,[11] N3 atom protonation (structure **C** in Scheme 1) is also possible. So, a total of three different types of tautomeric forms (**A** to **C**) have been used for the compounds with the common core structure depicted in Scheme 1.

It is crucial to correctly assign the molecular structures of this important type compounds (with the hydrogen atom on the right site) for structure-based drug design and discovery, as the binding of a drug target (say protein) with different tautomeric forms would be remarkably different for these compounds. If a wrong site was assigned for the hydrogen, the structure-based computational design would be meaningless and, therefore, could be misleading. A meaningful structure-based drug design and discovery must be based on the reliable structural assignment.

From thermodynamic point of view, all of these three types of tautomeric forms (**A** to **C** in Scheme 1) could coexist in solution, but with different relative concentrations. The question is which type of tautomeric form is dominant or more favorable in solution. In order to address this crucial question, we first performed first-principles electronic structure calculations on the molecular structures and energetics of four representative compounds (**1** to **4** in Scheme 1). The first-principles electronic structure calculations were performed on all of the three possible types of tautomeric forms for each of these four compounds. The computational results led to the prediction of the most favorable type of tautomeric form. To test the computational prediction, compound **4** was synthesized and its structure was characterized by X-ray diffraction technology, ^{1}H NMR, and IR spectrum. The combined computational and experimental studies consistently demonstrate that the dominant type of tautomeric form is always **A** in the gas phase, solution, and crystal. The conclusive assignment of the proton for 6-oxy purine derivatives provides a solid basis for future structure-based drug design and discovery associated 6-oxy purine derivatives.

Computational and Experimental Methods

Computational modeling

The initial structures of all compounds were built with GaussView 3.0. All of the molecular geometries were first optimized by using the density functional theory (DFT) with the B3LYP functional and the 6-31G* basis set. Harmonic vibrational frequency analysis was performed at the same level of theory (B3LYP/6-31G*) to make sure that each geometry optimized is indeed associated with a local minimum on the potential energy surface and to estimate the thermal correction to Gibbs free energy in the gas phase. Then the optimized geometries were employed to performed single-point energy calculations at the B3LYP/6-311++G** level.

The geometries optimized in the gas phase were also used as the initial structures for further geometry optimizations in aqueous solution using self-consistent reaction field (SCRF) theory at the B3LYP/6-31G* level. The quantum Onsager solvation model[12] was chosen for the geometry optimizations in aqueous solution (with a dielectric constant of 78.5). The radius of the cavity used in the quantum Onsager model was estimated from the molecular volume calculation at the B3LYP/6-31G* level on the gas phase geometry. The geometry optimization was followed by the harmonic vibrational frequency calculation at the same SCRF level of

theory for the thermodynamic correction to the Gibbs free energy in aqueous solution. Further, the geometries optimized in aqueous solution were employed to calculate the solvent shifts of the free energies by using the surface and volume polarization for electrostatic (SVPE)13,14, 15 implemented recently in Gaussian03 program.16 The SVPE model is also known as Fully Polarizable Continuum Model (FPCM),[17–24] because it fully account for both surface and volume polarization effects in determination of the solute-solvent electrostatic interaction. Finally, the non-electrostatic contributions to the solvation free energy of the solutes were estimated semi-empirically by using IEFPCM model25 implemented in the Gaussian03 program.

The SVPE calculations were carried out by using a local version16 of Gaussian03 program[26] on a 34-processors IBM Linux cluster in our own laboratory. All of the other calculations were performed using the Gaussian03 program on an IBM supercomputer (X-series Cluster with 340 nodes or 1,360 processors) at University of Kentucky Center for Computational Sciences.

Experimental details

Triethyl orthoformate, 2-cyano-2-amino-acetamide, and other chemical reagents were commercially available. Solvents were dried in a routine way and redistilled. ^{1}H NMR spectrum was recorded at 400 MHz in DMSO on a Varian 400 MHz NMR spectrometer. Mass spectrum was determined using a Trace MS 2000 organic mass spectrometry. Melting points were recorded on a Buchi B-545 melting point apparatus. Elemental analysis (EA) was carried out with a Vario EL III CHNSO elemental analyzer. The crystal structure of the title compound was determined on the Bruker Smart Apex CCD X-ray instrument.

Compound 4 was prepared by using a route (Scheme 2) modified from what described in literature.[27]

At room temperature, 1.02 g (56 mmol) methyl 3-methoxyphenyl acetate and 0.24 g (14 mmol) 5-amino-1-(2-hydroxyethyl)-1H-imidazole-4-carboxamide (**5**) were desolved in 10 mL warm pure methanol to obtain a solution (solution A), and 0.15 g (63 mmol) sodium was desolved in 10 mL pure methanol to obtain another solution (solution B). Then, the mixture of the solutions A and B was heated under refluxing for 15 h. The methanol was distilled off using a rotary evaporator, and then 30 mL water was added to the residue and the mixture was extracted by dichloromethane (3×40 mL). During the extraction, the product was precipitated out, and filtration by suction and silica gel chromatograph to give 0.32 g compound **4** (yield 76%) as a white solid (melting point: 199.1 °C). Compound **4** was characterized by ^{1}H NMR and IR. IR (KBr/cm^{-1}): 3313 (N-H), 3089, 2950, 2841, 1673 (C=O), 1589, 1535, 1475, 1436, 1378, 1260, 1186, 1167, 1076, 1048, 1034, 875, 767, 710, and 648; EI-Ms : m/z (%) 300.1 (M^+,86.11), 269.2 (100.00), 255.1 (64.16), 109.1 (86.43), 91.1 (43.17), 77.1 (45.45), 65.1 (27.19), and 45.2 (41.11); ^{1}H NMR (400MHz, DMSO-d_6) δ: 12.32 (s,NH,1H), 7.96 (s,CH, 1H), 6.80–7.24 (m,ArH,4H), 4.98 (t,OH,1H,^{2}J=5.6 Hz), 4.14 (t,CH_2,2H, ^{2}J=5.2 Hz), 3.94 (s,CH2,2H), and 3.32–3.75 (m,5H,OCH_3,CH_2); Anal. calcd for C15H16N4O3: C, 59.99; H, 5.37; N, 18.66; O, 15.98. Found: C, 59.96; H, 5.34; N, 18.98.

For the purpose of determining an X-ray crystal structure, a single crystal of compound **4** suitable for X-ray analysis was grown from methanol at 293 K. The crystal structure was determined by X-ray crystallography and the determined crystal structure was shown in Figure 2. Crystal data obtained for compound **4**: Triclinic; a = 7.2840(10) Å, b = 8.9089(12) Å, c = 13.7793(19) Å, β= 76.153(2)°; V = 843.7(2) Å^3, T = 295(2) K, Space group P-1, Z=8, Dc = 1.308 g/cm^3, μ(Mo-Kα) = 0.096 mm^{-1}, F(000) = 352. 5660 reflections measured, 3439 unique, R(int) = 0.0511, which were used in all calculation. Fine R1 = 0.0532, wR2 = 0.1316 R1 = 0.0805, wR2 = 0.1594 (all data).

Results and Discussion

Geometries and energetics from first-principles electronic structure calculations

The geometries of various tautomeric forms of compounds **1** to **4** optimized in the gas phase are depicted in Figure 1. Table 1 collects the key bond lengths in the optimized geometries. The corresponding bond lengths optimized in aqueous solution are also listed in Table 1 for comparison. As one can see in Table 1, the optimized bond lengths in the gas phase are all very close to the corresponding values optimized in aqueous solution. The largest difference is ~0.01 Å. For convenience, the discussion below will only refer to the geometries optimized in aqueous solution, unless explicitly indicated otherwise.

As one can see in Table 1, the optimized geometric parameters for different tautomeric forms are remarkably different. However, for a given type of tautomeric form, the optimized bond length values for each bond in different compounds are very close. In the optimized geometries of tautomeric form **A** of compounds **1** to **4**, the C6-O10 bond length is 1.222 to 1.223 Å, the C6-N1 bond length is 1.430 to 1.434 Å, and the C2-N3 bond length is 1.301 to 1.309 Å. In the optimized geometries of tautomeric form **B** (including conformations **B-1** and **B-2**) of compounds **1** to **4**, the C6-O10 bond length is 1.342 to 1.351 Å, the C6-N1 bond length is 1.325 to 1.333 Å, and the C2-N3 bond length is 1.331 to 1.340 Å. In the optimized geometries of tautomeric form C of compounds **1** to **4**, the C6-O10 bond length is 1.224 to 1.230 Å, the C6-N1 bond length is 1.421 to 1.427 Å, and the C2-N3 bond length is 1.373 to 1.383 Å. The largest difference between different compounds for a given bond length does not exceed 0.01 Å. So, the substituent effects on the bond lengths are all rather small.

In order to determine the most favorable tautomeric form (**A**, **B**, or **C**) of 6-oxy purine derivatives, we calculated the relative Gibbs free energies and calculated energetic results are summarized in Table 2. For all compounds examined, tautomer **A** is always associated with the lowest Gibbs free energy in both the gas phase and solution. The Gibbs free energies of the other tautomers are significantly higher, particularly for the results calculated in solution. Thus, the computational data predict that 6-oxy purine derivatives should dominantly exist in tautomer **A**, and the other tautomers are negligible in solution.

Results from wet experimental studies

To test the computational prediction, compound **4** was selected for wet experimental study. The target compound was synthesized *via* the route outlined in Scheme 2, and characterized by ^{1}H NMR, elemental analysis, mass spectroscopy, and IR spectrum. Methyl 3-methoxy-phenylacetate was obtained by 3-methoxy-phenylacetic acid with absolute methanol under the present of the catalyst concentrated sulfuric acid in 96% yield. The intermediate 5-amino-1-(2-hydroxyethyl)-1H-imidazole-4-carboxamide (**5**) was prepared according to the procedure described by Banerjee *et al.*[28], but we modified the procedure by adding pyridine as a catalyst to increase the yield from 42% (reported by Banerjee *et al*.) to 73.2% (this work). The ^{1}H NMR spectrum of **5** was consistent with that reported in the literature.[28] The compound **4** was obtained by refluxing intermediate **5** with methyl 3-methoxyphenyl acetate under CH3ONa/CH3OH system.

The main difference between tautomers **A**, **B**, and **C** lies in the position of a hydrogen atom which can bond to N1, O10, or N3. Since the chemical environments of a hydrogen atom on N1, O10, and N3 are different, one might expect to use nuclear magnetic resonance (NMR) techniques to determine the position of the hydrogen atom. On the ^{1}H NMR spectrum (see supporting information) of compound **4**, a single peak at 12.32 ppm (1H) was found. This absorption is attributed to the resonance of the hydrogen atom on –NH or –OH group. However,

as each of the three possible tautomers, *i.e.* **4A, 4B** (**4B-1** or **4B-2**), and **4C**, has a –NH or –OH group, it is difficult to determine which tautomer is the right one for compound **4**.

X-ray diffraction technique is a powerful tool to determine molecular structures. Figure 2 depicts the intermolecular interaction in the X-ray crystal structure of compound **4**. Since X-ray diffraction itself cannot directly determine the positions of hydrogen atoms, only heavy atoms are shown in Figure 2. As shown in Figure 2, N1 atom in one molecule is only ~2.8 Å away from O10 atom of the other molecule in the X-ray crystal structure. There must be a hydrogen atom between N1 atom of one molecule and O10 atom of the other molecule of compound **4**. In other words, the hydrogen atom to be assigned should covalently bond to either N1 or O10 atom in compound **4**. So, in the X-ray crystal structure, only tautomers **A** and **B** are possible, and tautomer **C** can be excluded. Further, the C6-O10, C6-N1, and C2-N3 bond lengths in the X-ray crystal structure are 1.242, 1.390, and 1.303 Å, respectively. The C6-O10 bond length of 1.242 Å clearly reveals that the C6-O10 bond should be a typical C=O double bond, suggesting that the hydrogen atom to be assigned should covalently bond to N1 atom, rather than O10 atom, in compound **4**. In other words, the tautomer observed in the X-ray crystal structure should be **A**. As seen in Table 1, within all of the optimized geometries of compound **4**, only tautomer A has all bond lengths consistent with the corresponding experimental values. The C6-O10, C6-N1, and C2-N3 bond lengths in the optimized geometry of **4A** are 1.222, 1.430, and 1.309 Å, respectively, in good agreement with the corresponding bond lengths in the X-ray crystal structure.

It is possible that the tautomer observed in an X-ray crystal structure is not necessarily the most favorable tautomer in solution. This is because different tautomers may have different intermolecular interactions (including hydrogen bonding) and, thus, may be associated with different crystal packing forces. For this reason, a slightly less favorable tautomer with a much more favorable force could be crystallized. Nevertheless, our conclusion of the most favorable tautomer **4A** is strongly supported by the fact that our determined X-ray crystal structure is completely consistent with the computationally determined tautomer with the lowest free energy.

Tautomer **A** determined by the X-ray structural analysis was supported further by IR spectrum of compound **4**. On the IR spectrum (see supporting information), there was a strong absorption at 1673 cm^{-1} which should be attributed to the stretching vibration of a carboxyl (C=O) bond in amide. As C6-O10 is the only candidate for this type of carboxyl bond in the compound, the IR spectrum can exclude tautomer **B** and, thus, supports tautomer **A**.

Conclusion

First-principles electronic structure studies on the possible tautomeric forms (**A, B,** and **B**) and their relative stability of four representative 6-oxy purine derivatives (compounds **1** to **4**) have demonstrated that the most favorable type of tautomeric form of these compounds in both the gas phase and aqueous solution should always be **A** in which a hydrogen atom bonds with N1 atom on the purine ring. To examine the computational results, one of the 6-oxy purine derivatives (*i.e.* compound **4**) has been synthesized and its structure has been characterized by X-ray diffraction and ^{1}H NMR and IR spectroscopy. All of the obtained computational and experimental data are consistent with the conclusion that the 6-oxy purine derivative exists in tautomer **A**. The conclusive structural assignment is expected to be valuable for future computational studies on 6-oxy purine derivative binding with proteins and for computational drug design involving this type of compounds.

Supplementary Material

Refer to Web version on PubMed Central for supplementary material.

Acknowledgments

The research was supported in part by National Institutes of Health (grant RC1MH088480) and National Natural Science Foundation of China (grants 20602014, 20503008, and 20372023). The authors also acknowledge the Center for Computational Sciences (CCS) at University of Kentucky for supercomputing time on IBM X-series Cluster with 340 nodes or 1,360 processors.

References

1. Cornaglia FP. Compounds endowed with immunomodulating activity. 1983 EP077460.
2. Michael MA, Cottam HB, Smee DF, Robins RK, Kini GD. J. Med. Chem 1993;36:3431. [PubMed: 8230133]
3. Tan TMC, Yang F, Fu H, Raghavendra MS, Lam Y. J. Comb. Chem 2007;9:210. [PubMed: 17348727]
4. Niewoehner U, Bischoff E, Schuetz H, Perzborn E, Schramm M. Preparation of 2,9-disubstituted purin-6-ones as antiinflammatories and cardiovascular agents. 1996 EP 722944.
5. Kelley JL, Linn JA, Selway JWT. J. Med. Chem 1989;32:218. [PubMed: 2535875]
6. Yamazaki A, Kumashiro I, Takenishi T. J. Org. Chem 1967;32:3258.
7. Zhang H-Z, Fried J. Synth. Commun 1996;26:351.
8. Isobe Y, Tobe M, Ogita H, Kurimoto A, Ogino T, Kawakami H, Takaku H, Sajiki H, Hirota K, Hayashi H. Bioorg. Med. Chem 2003;11:3641. [PubMed: 12901909]
9. Schaeffer HJ, Bhargava PS. Biochemistry 1965;4:71. [PubMed: 14285247]
10. Montgomery JA, Thomas HJ. J. Org. Chem 1965;30:3235.
11. Costas ME, Acevedo-Chavez R. J. Phys. Chem. A 1997;101:8309.
12. Wong MW, Frisch MJ, Wiberg KB. J. Am. Chem. Soc 1991;113:4776.
13. Zhan C-G, Bentley J, Chipman DM. J. Chem. Phys 1998;108:177.
14. Zhan C-G, Chipman DM. J. Chem. Phys 1998;109:10543.
15. Zhan C-G, Chipman DM. J. Chem. Phys 1999;110:1611.
16. Vilkas MJ, Zhan C-G. J. Chem. Phys 2008;129 194109/1.
17. Zhan C-G, Dixon DA. J. Phys. Chem. A 2001;105:11534.
18. Dixon DA, Feller D, Zhan C-G, Francisco JS. J. Phys. Chem. A 2002;106:3191.
19. Zheng F, Zhan C-G, Ornstein RL. J. Phys. Chem. B 2002;106:717.
20. Zhan C-G, Dixon DA. J. Phys. Chem. A 2002;106:9737.
21. Zhan C-G, Spencer P, Dixon DA. J. Phys. Chem. B 2003;107:2853.
22. Lu H, Chen X, Zhan C-G. J. Phys. Chem. B 2007;111:10599. [PubMed: 17691837]
23. Chen X, Zhan C-G. J. Phys. Chem. A 2004;108:3789.
24. Chen X, Zhan C-G. J. Phys. Chem. B 2008;112:16851. [PubMed: 19367986]
25. Cances E, Mennucci B, Tomasi J. J. Chem. Phys 1997;107:3032.
26. Frisch MJT, GW.; Schlegel, HB.; Scuseria, GE.; Robb, MA.; Cheeseman, JR.; Montgomery, JA., Jr; Vreven, T.; Kudin, KN.; Burant, JC.; Millam, JM.; Iyengar, SS.; Tomasi, J.; Barone, V.; Mennucci, B.; Cossi, M.; Scalmani, G.; Rega, N.; Petersson, GA.; Nakatsuji, H.; Hada, M.; Ehara, M.; Toyota, K.; Fukuda, R.; Hasegawa, J.; Ishida, M.; Nakajima, T.; Honda, Y.; Kitao, O.; Nakai, H.; Klene, M.; Li, X.; Knox, JE.; Hratchian, HP.; Cross, JB.; Adamo, C.; Jaramillo, J.; Gomperts, R.; Stratmann, RE.; Yazyev, O.; Austin, AJ.; Cammi, R.; Pomelli, C.; Ochterski, JW.; Ayala, PY.; Morokuma, K.; Voth, GA.; Salvador, P.; Dannenberg, JJ.; Zakrzewski, VG.; Dapprich, S.; Daniels, AD.; Strain, MC.; Farkas, O.; Malick, DK.; Rabuck, AD.; Raghavachari, K.; Foresman, JB.; Ortiz, JV.; Cui, Q.; Baboul, AG.; Clifford, S.; Cioslowski, J.; Stefanov, BB.; Liu, G.; Liashenko, A.; Piskorz, P.; Komaromi, I.; Martin, RL.; Fox, DJ.; Keith, T.; Al-Laham, MA.; Peng, CY.; Nanayakkara, A.; Challacombe, M.; Gill, PMW.; Johnson, B.; Chen, W.; Wong, MW.; Gonzalez, C.; Pople, JA. Revision A.1 ed. Pittsburgh, PA: Gaussian, Inc.; 2003. Gaussian 03.

27. Pamukcu R, Piazza GA. Preparation of 9-substituted 2-(2-alkoxyphenyl)purin-6-ones as neoplasm inhibitors. 2000 US6124303.

28. Banerjee T, Chaudhuri S, Moore M, Ray S, Chatterjee PS, Roychowdhury P. J. Chem. Crystallogr 1999;29:1281.

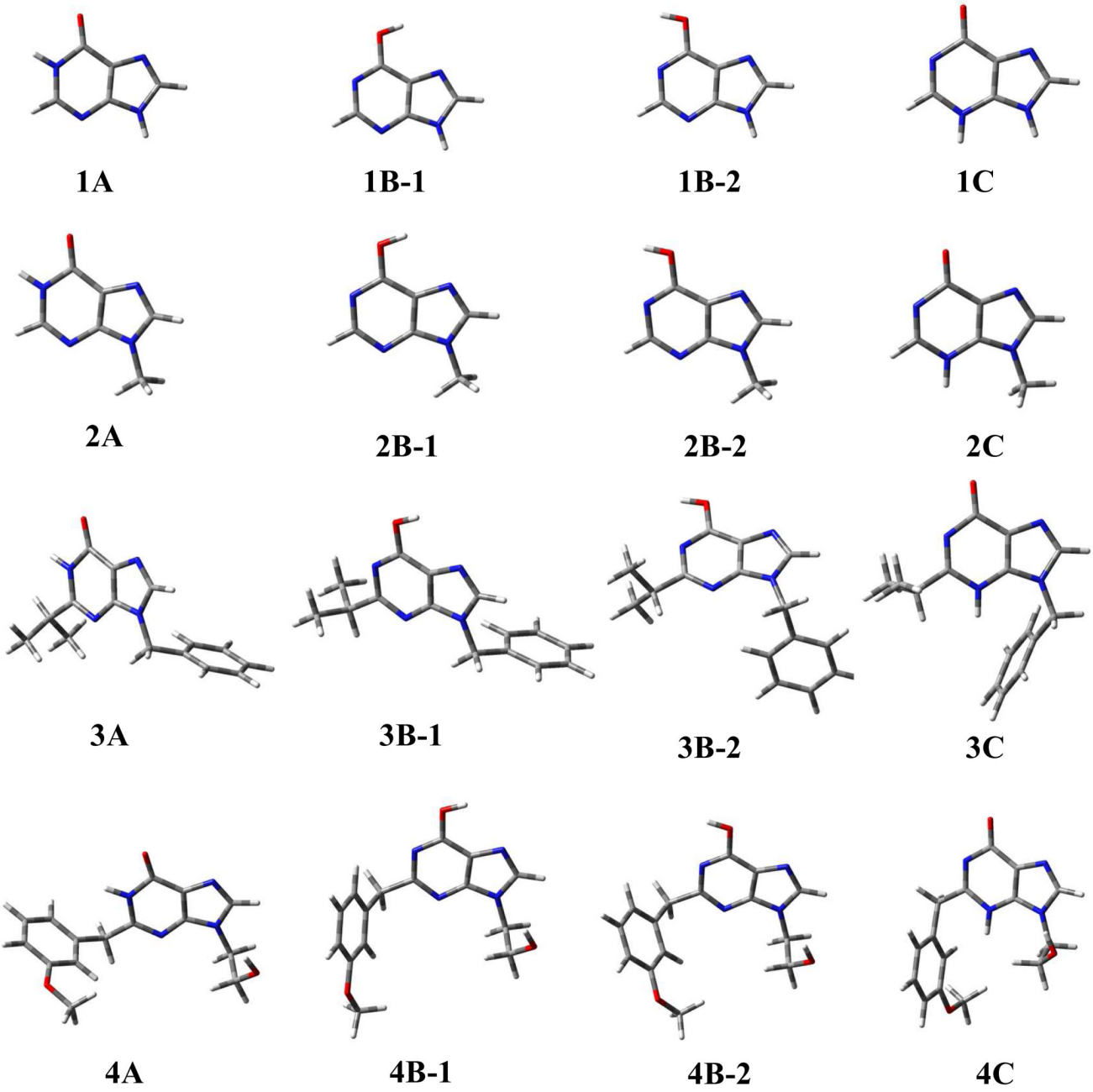

Figure 1.
Geometries optimized at the B3LYP/6-31G* level for the three possible types of tautomeric forms of 6-oxy purin derivatives (compounds **1** to **4**). Color codes: red, oxygen; blue, nitrogen; gray, carbon; white, hydrogen.

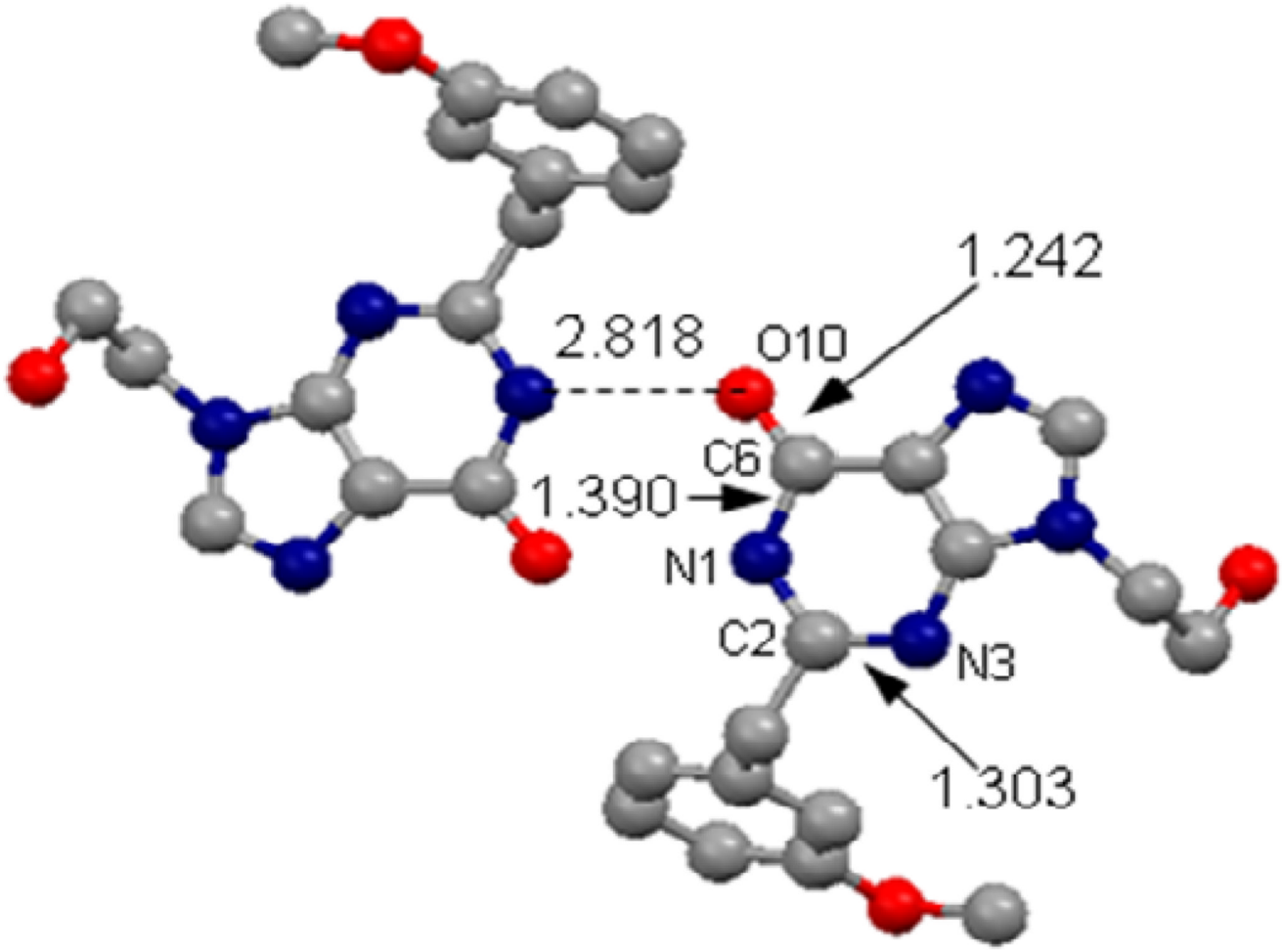

Figure 2.
Intermolecular interaction in the X-ray crystal structure of compound **4**. Color codes: red, oxygen; blue, nitrogen; gray, carbon.

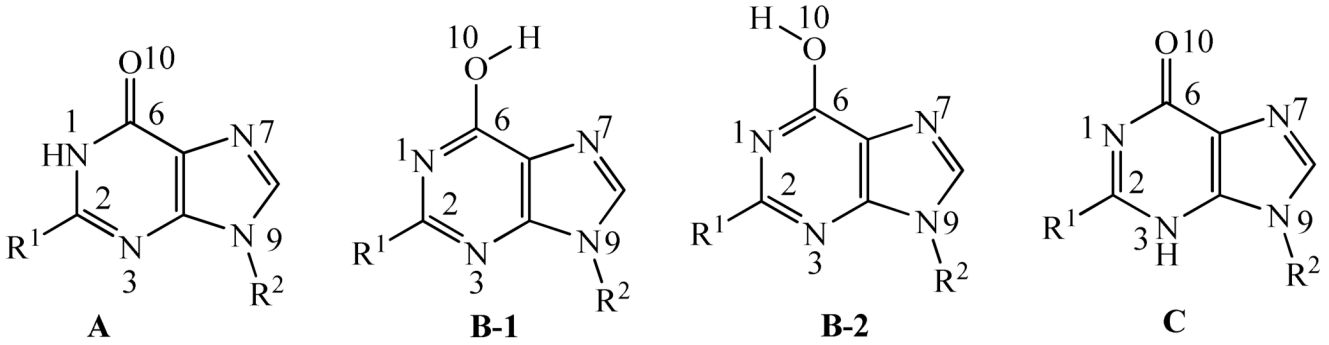

Compound **1**: R^1=H, R^2 =H
Compound **2**: R^1=H, R^2 =CH_3
Compound **3**: R^1=i-Pr, R^2=benzyl
Compound **4**: R^1=3-methoxybenzyl, R^2=CH_2CH_2OH

Scheme 1.
Three possible types of tautomeric forms of 6-oxy purine derivatives; tautomer **B** may take two different types of conformations (**B-1** and **B-2**).

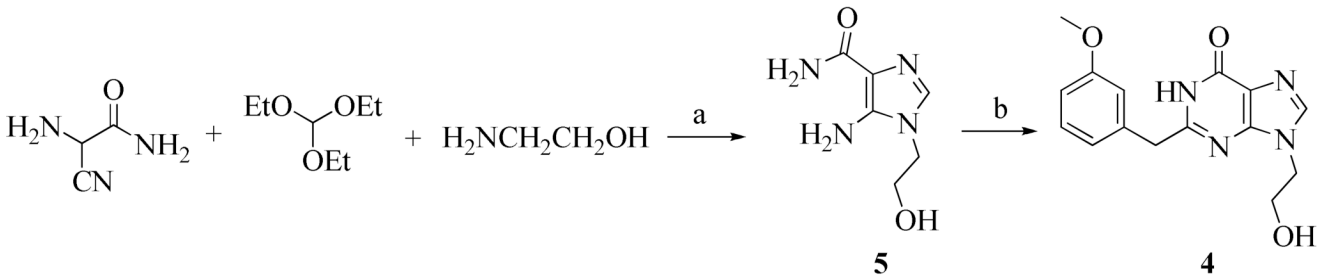

Scheme 2.

Synthesis of compound **4**. Reagents and conditions: (a) pyridine, acetonitrile, reflux 1 h and then 15 min; (b) methyl 3-methoxyphenyl acetate, CH_3ONa, reflux.

Table 1

Key bond lengths (in Å) in the geometries optimized for various possible structures of compounds **1** to **4**, in comparison with the corresponding experimental values in the X-ray crystal structure of compound **4**.

Structure[a]	r(C6-O10)	r(C6-N1)	r(C2-N3)
1A	1.217 (1.223)	1.436 (1.431)	1.303 (1.301)
1B-1	1.344 (1.349)	1.328 (1.329)	1.338 (1.335)
1B-2	1.339 (1.344)	1.333 (1.333)	1.333 (1.331)
1C	1.216 (1.228)	1.436 (1.426)	1.386 (1.375)
2A	1.218 (1.223)	1.437 (1.433)	1.303 (1.301)
2B-1	1.344 (1.351)	1.328 (1.329)	1.337 (1.334)
2B-2	1.340 (1.346)	1.334 (1.333)	1.332 (1.331)
2C	1.216 (1.230)	1.436 (1.427)	1.385 (1.373)
3A	1.219 (1.222)	1.438 (1.434)	1.309 (1.309)
3B-1	1.346 (1.350)	1.324 (1.325)	1.342 (1.340)
3B-2	1.341 (1.344)	1.330(1.330)	1.338 (1.337)
3C	1.218 (1.227)	1.428 (1.421)	1.388 (1.380)
4A	1.218 (1.222)	1.435 (1.430)	1.309 (1.309)
4B-1	1.345 (1.348)	1.326 (1.326)	1.341 (1.340)
4B-2	1.340 (1.342)	1.331 (1.330)	1.338 (1.337)
4C	1.217 (1.224)	1.431 (1.425)	1.387 (1.383)
4 (expt.)[b]	1.242	1.391	1.303

[a] Unless indicated otherwise, all of the geometries were optimized at the B3LYP/6-31G* level in the gas phase. The values in parentheses were optimized at the B3LYP/6-31G* level in aqueous solution.

[b] Bond lengths in the X-ray crystal structure of compound **4**.

Table 2

Calculated relative Gibbs free energies (ΔG in kcal/mol) of different molecular structures/conformations of compounds **1** to **4**.[a]

Compound	Phase	Structures			
		A	B-1	B-2	C
1	ΔG(gas)	0.0	5.4	4.0	18.9
	ΔG(sol)	0.0	10.2	9.1	8.5
2	ΔG(gas)	0.0	5.0	3.8	19.7
	ΔG(sol)	0.0	11.4	8.8	9.4
3	ΔG(gas)	0.0	7.5	5.3	18.6
	ΔG(sol)	0.0	10.7	9.8	12.0
4	ΔG(gas)	0.0	5.8	4.9	18.9
	ΔG(sol)	0.0	11.7	8.0	8.1

[a]The energy calculations were performed at B3LYP/6-311++G** level by using geometries optimized at the B3LYP/6-31G* level. Thermal corrections to Gibbs free energies were estimated at the B3LYP/6-31G* level.